Journal of Asian Earth Sciences 56 (2012) 218–228

Contents lists available at SciVerse ScienceDirect

Journal of Asian Earth Sciences

journal homepage: www.elsevier.com/locate/jseaes

Zoning of mineralization in hypogene porphyry copper deposits: Insight from comb microfractures within quartz–chalcopyrite veins in the Hongshan porphyry Cu deposit, western Yunnan, SW China

Xing-Wang Xu [a,b,*], Bao-Lin Zhang [a], Guang-He Liang [a], Ke-Zhang Qin [a,b]

[a] Key Laboratory of Mineral Resources, Institute of Geology and Geophysics, Chinese Academy of Sciences, Beijing 100029, People's Republic of China

[b] Xinjiang Research Center for Mineral Resources, Chinese Academy of Sciences, Urumqi 830011, People's Republic of China

ARTICLE INFO

Article history:
Received 9 July 2011
Received in revised form 1 May 2012
Accepted 21 May 2012
Available online 26 May 2012

Keywords:
Comb microfractures
Volume expansion
Crystallization
Zoning of mineralization
Hypogene porphyry copper deposits

ABSTRACT

The origin of zonal mineralization in porphyry copper deposit is important for understanding the mineralization processes. We propose a new, modified "orthomagmatic" genetic model for mineralization zoning in hypogene porphyry copper deposits. This new model is based on the features and formation mechanism of comb microfractures in quartz–chalcopyrite veins within pyrite vein from the Hongshan porphyry copper deposit in Zhongdian County, western Yunnan Province, SW-China. The main evidence for this model is volume expansion related to crystallization of chalcopyrite, magnetite and K-metasomatism in the deposit.

Comb microfractures are well developed in quartz–chalcopyrite veins and are present as comb-quartz veinlets consisting of a zone of central longitudinal quartz overprinted by laterally grown quartz combs. Chalcopyrite fragments lie perpendicular to the central quartz veinlet and were dismembered by the quartz combs. The combed microfractures are typical tensional hydrofractures. The formation of the comb microfractures is related to volume expansion that was induced by crystallization of chalcopyrite from a chalcopyrite melt that resulted in the subsequent increase of volumetric pressure in the confined residual silica melt. The formation mechanism of the comb microfractures, including volume expansion induced by crystallization, increases volumetric pressure, hydrofracturing and fluid expulsion, and was the most likely process for zoning of minerals in hypogene porphyry copper deposits.

Fabrics in the veins and veinlets are consistent with overpressuring and injection and are common structures that are directly related to volumetric pressure and crystallization of chalcopyrite and magnetite and K-metasomatism in hypogene porphyry copper deposits. The volume expansion ratio of chalcopyrite mineral to melt and that of magnetite mineral to melt are approximately 19 vol.% and 20 vol.%, respectively. The volume expansion rate of a monomolecular lattice is $\geqslant$8 vol.% for orthoclase replacing plagioclase.

We suggest that zoning of mineralization in hypogene porphyry copper deposits is mainly related to hydrofracturing, migration and distribution of ore-forming fluids, including (1) the enclosure and formation of a mush core, (2) concentration of ore-forming fluids in the orthoclase shell, (3) K-metasomatism and pressure building, (4) hydrofracturing and migration of ore-forming fluids, and (5) prior crystallization of magnetite and chalcopyrite that will expel residual fluids upwards and outwards due to the change in volumetric pressure.

1. Introduction

Porphyry copper deposits supply nearly three-quarters of the world's copper (Sillitoe, 2010). These deposits are characterized by alteration and mineralization mineral zoning. This hypogene zoning typically manifests as quartz and pyrite in an outer phyllic zone, and K-feldspar and chalcopyrite in an inner alteration zone (e.g., Nielsen, 1968; Lowell and Guilbert, 1970; Corn, 1975; Cooke et al., 2005). The origin of mineral zoning in hypogene porphyry copper deposits has been related to a number of physical and chemical controls, such as: (1) temperature gradients, with near-magmatic temperatures at the center of the stock, grading to relatively cool temperatures in the wall rocks (Park, 1955, 1957; Nielsen, 1968); (2) chemical gradients and titration related to solubility of metallic compounds in the ore-forming solution (Barnes, 1962),

* Corresponding author at: Xinjiang Research Center for Mineral Resources, Chinese Academy of Sciences, Urumqi 830011, People's Republic of China. Tel.: +86 10 82998198; fax: +86 10 62010846.

E-mail address: xuxw@mail.iggcas.ac.cn (X.-W. Xu).

1367-9120/$ - see front matter
http://dx.doi.org/10.1016/j.jseaes.2012.05.017

related to temperature, pH, total chloride and pressure (Hemley et al., 1992a,b); (3) variation in the ratio of common metal cations to hydrogen ions in fluids (Hemley and Jones, 1964; Fournier, 1967b; Beane and Bodnar, 1995), which is probably related to mixing of magmatic fluid with meteoric water (Nielsen, 1968; Lowell and Guilbert, 1970); (4) magma oxidation state (oxygen fugacity) (Candela, 1992, 1997; Williams et al., 1995; Rowins, 2000); and (5) partitioning coefficient of metals among silicate melts, vapor-facies, chloride-bearing aqueous fluids, and crystalline phases during crystallization (Candela, 1997; Halter et al., 2002; Williams-Jones and Heinrich, 2005). In these systems copper may be efficiently concentrated in vapor and moderate to highly saline aqueous phases, which move upwards to form porphyry copper systems at shallower depths than porphyry-Mo systems (Burnham and Ohmoto, 1980; Williams et al., 1995; Williams-Jones and Heinrich, 2005). These genetic models and concepts, however, cannot precisely predict the spatial distribution of alteration and mineralization with respect to a cylindrical magmatic stock. An example is the common occurrence of abundant chalcopyrite and K-feldspar in the middle zones of porphyry copper deposits instead of at the center of the stock in the Lowell and Guilberrt's model; therefore it is important to search for further explore for general mechanisms of formation. In this paper, we propose that volume pressure that was induced by crystallization and K-metasomatism is the most important contributor to spatial alteration and mineralization zoning in porphyry-Cu deposits. Comb microfractures filled with comb-like quartz within confined quartz–chalcopyrite veins were identified in the course of this study in the Hongshan porphyry copper deposit, western Yunnan, SW-China. These textures provide evidence, which suggests that crystallization of chalcopyrite mineral from a chalcopyrite–silica melt—an important compound in ore-forming fluids from porphyry copper deposits—was caused by volume expansion. Volume expansion can potentially raise the pressure within the rock-fluid system enough to create fractures and drive hydrous silica melt outwards to produce theoretical and observed mineral zoning in most porphyry copper deposits. Examination and analysis of the porphyry magma and the volume varieties observed in many mineralization systems and specifically the Hongshan Cu-polymetallic deposit during alteration and solidification processes, allows the construction of a new genetic model for mineralization zoning in porphyry copper deposits.

2. Geological setting

The Hongshan Cu-polymetallic deposit is approximately 30 km NE of Zhongdian County in eastern Tibet (Fig. 1a). The deposit lies within the western part of the Yangtze tectonic Plate adjacent to the north northwest-striking Jinshajiang suture (Fig. 1a). The latter is a major shear zone containing a large number of both Triassic Cu–Mo porphyry deposits and Tertiary Cu–Mo–Au porphyry deposits. The Triassic porphyries and associated Cu–Mo porphyry deposits in the Zhongdian area have ages ranging from 240 to 210 Ma, and are attributed to subduction of the Paleo-Tethyan (Jinshajiang) oceanic plate (Zhao, 1995; Zeng et al., 2003, 2004, 2006). Tertiary porphyritic bodies and associated Cu–Mo–Au deposits lie in the northwest Yulong area (Rui et al., 1984; Zhang et al., 1998;

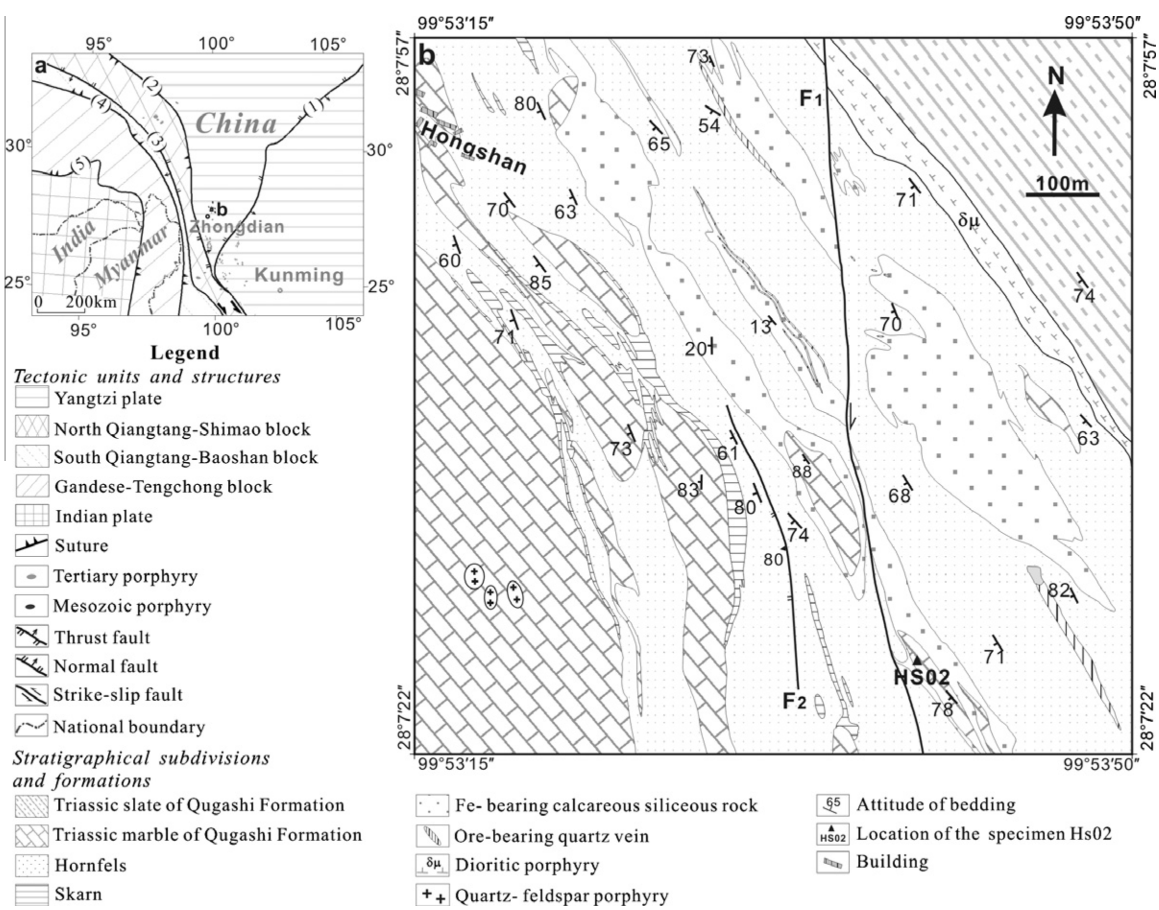

Fig. 1. (a) Regional tectonic location and (b) geological map of the Hongshan porphyry Cu deposit, western Yunnan, SW-China (revised after Xu et al.(2006a, 2007a)). (1) Rongmenshan thrust fault, (2) Jinshajiang suture, (3) Langchangjian thrust fault, (4) Nujiang suture, (5) Yarlungzangbojiang suture.

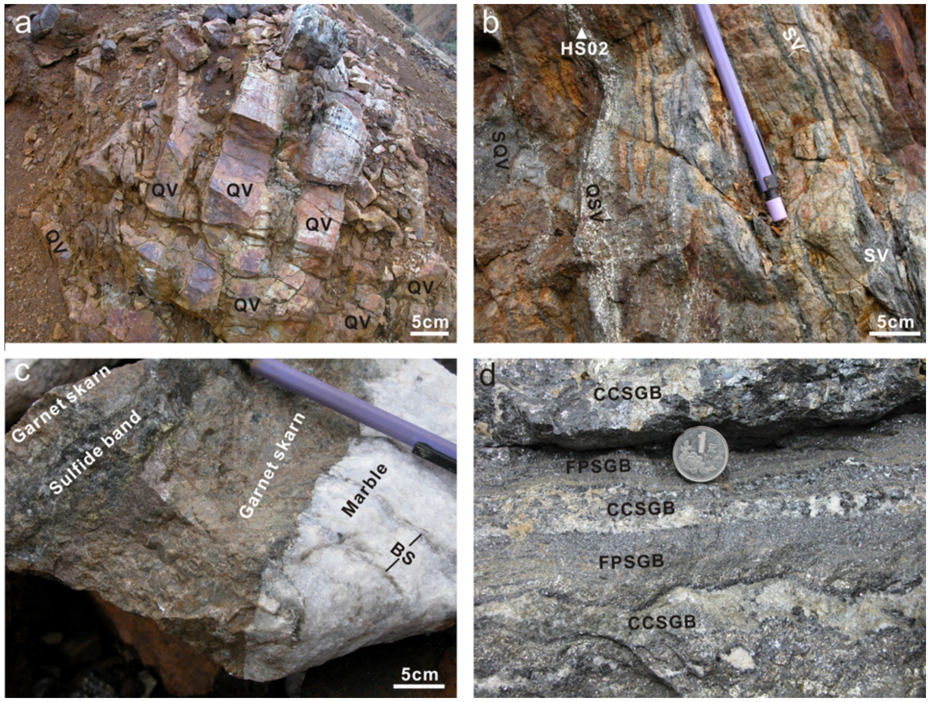

Fig. 2. Photographs showing quartz–sulfide veinlets (a and b) and banded polymetallic skarn ores (c and d). Sulfide veinlets (SV), quartz–sulfide veinlets (QSV) and sulfide–quartz veinlets (SQV) in image b were filled along fractures in altered marble. The white triangle in image b shows location of the sample HS02. The sulfide band between garnet skarn bands in image c was consisted of chalcopyrite, pyrrhotite and magnetite, and contact plane between garnet skarn and marble in image c was nearly perpendicular to bedding structures (BS). Sulfide bands in image d were varied laterally both in composition and grain size, containing coarse calcite–sphalerite–galena band (CCSGB) and fine pyrite–sphalerite–galena band (FPSGB). Diameter of the coin in image d is about 2 cm.

Hou et al., 2003, 2007), in the Zhongdian area (Yang et al., 2002), and to the southeast in the Jianchun and the Dali areas (Hu et al., 1997; Peng et al., 1998; Xu et al., 2007a,b). They formed between 65 and 3.6 Ma (Xu et al., 2006b,c,d), with peak magmatic activity occurring between 40 and 30 Ma (Chung et al., 1998; Wang et al., 2001; Guo et al., 2005; Xu et al., 2007c). The Tertiary Cu–Mo–Au porphyry deposits are most likely related to bi-directional resubduction of the buried Jinshajiang Paleo-Tethys oceanic crust resulting from Tertiary India-Asia collision (Xu et al., 2007a).

Bedrock in the Hongshan district consists of upper Triassic Qugasi Formation marble and slate, as well as hornfels, skarn, dioritic-porphyry, quartz veins, and calcareous siliceous rocks (Fig. 1b). Slate is present in the northeastern part of the Hongshan district, diorite porphyry is located to the west of the slate, and the marble is present in the central to western parts of the district (Fig. 1b). Lithologies are uniclinal, striking NW 310° and dipping SW at 60–90°. The calcareous siliceous rocks lie unconformably above marble, hornfels, skarn and a magnetite–pyrrhotite body with a distinct *contact zone* containing some ore-bearing quartz veins in the middle of the Hongshan district. Three irregular ellipsoid, quartz–feldspar porphyritic stocks, each <50 m long in plan view, with a whole-rock Rb–Sr age of about 216 Ma (Yunnan Bureau of Geology and Mineral Resources, 1990) lie in the western parts of the Hongshan district. Some buried molybdenite- bearing, layered or lenticular granite-porphyry bodies also are present in deeper areas in the central part of the district. Six molybdenite specimens from the ore-bearing quartz veins were dated using Re–Os isotopes. These samples have model ages between 75.46 and 78.46 Ma and an isochron age of about 77 Ma (Xu et al., 2006a), implying that the granitic porphyritic Cu deposit in the Hongshan area formed in the late Cretaceous. Faults in the Hongshan district are mainly NNW-trending thrust strike-slip faults.

The Hongshan Cu-polymetallic deposit contains more than 20 orebodies positioned within five ore alignments that in total contain 0.23 Mt Cu, 11,086 t Pb, 14,176 t Zn, 5759 t Mo, and 193 t W (SGSTYBGMR, 1971). Ore minerals include chalcopyrite, pyrrhotite, pyrite, sphalerite, galena, bornite, tetrahedrite, bismuthinite, molybdenite, scheelite, and magnetite. There are mainly two types of mineralization: quartz–sulfide veinlets (Fig. 2a and b), and banded polymetallic skarn ores (Fig. 2c and d). The massive skarn ores lie along the contact zone of the Triassic quartz-feldspar porphyry, whereas the quartz–sulfide veins are genetically related to a later Cretaceous granite-porphyry (Xu et al., 2006a). The ore-forming fluids were trapped in fluid inclusions in quartz veins in the Hongshan porphyry Cu deposit. The fluids are aqueous containing equivalent CH_4 and CO_2, and have $\delta^{18}O$, $\delta^{13}D$ and $\delta^{13}C$ values ranging from 3.76‰ to 5.20‰, from −83.15‰ to −89.75‰ and from 0.92‰ to −6.23‰ (Xu et al., 2006a), indicating that the ore-forming fluids for the porphyry-Cu mineralization system are magmatic and transitional between oxidized and reduced (Rowins, 2000).

3. Characteristics of comb microfractures

Comb microfractures within confined quartz–chalcopyrite veinlets (ore specimen HS02), in altered marble (Fig. 2b) in the southeastern part of the Hongshan Cu-polymetallic district (Fig. 1b) consist of pyrite (60 vol.%), pyrrhotite (10 vol.%), sphalerite (5 vol.%), galena (5 vol.%), chalcopyrite (5 vol.%), and quartz–chalcopyrite aggregates and veinlets, and quartz veinlets (Fig. 3a). Coarse-grained intergrowths of pyrrhotite, sphalerite and galena are embedded in pyrite as inclusions with round outlines (Fig. 3a), indicating that they formed under reduced conditions during an earlier crystallization of the quartz–sulfide veins. Pyrite contains fine disseminations of chalcopyrite <20 μm in diameter (Fig. 3b). A few chalcopyrite grains are oxidized to malachite (Fig. 3b and c). The quartz–chalcopyrite veinlets and their host

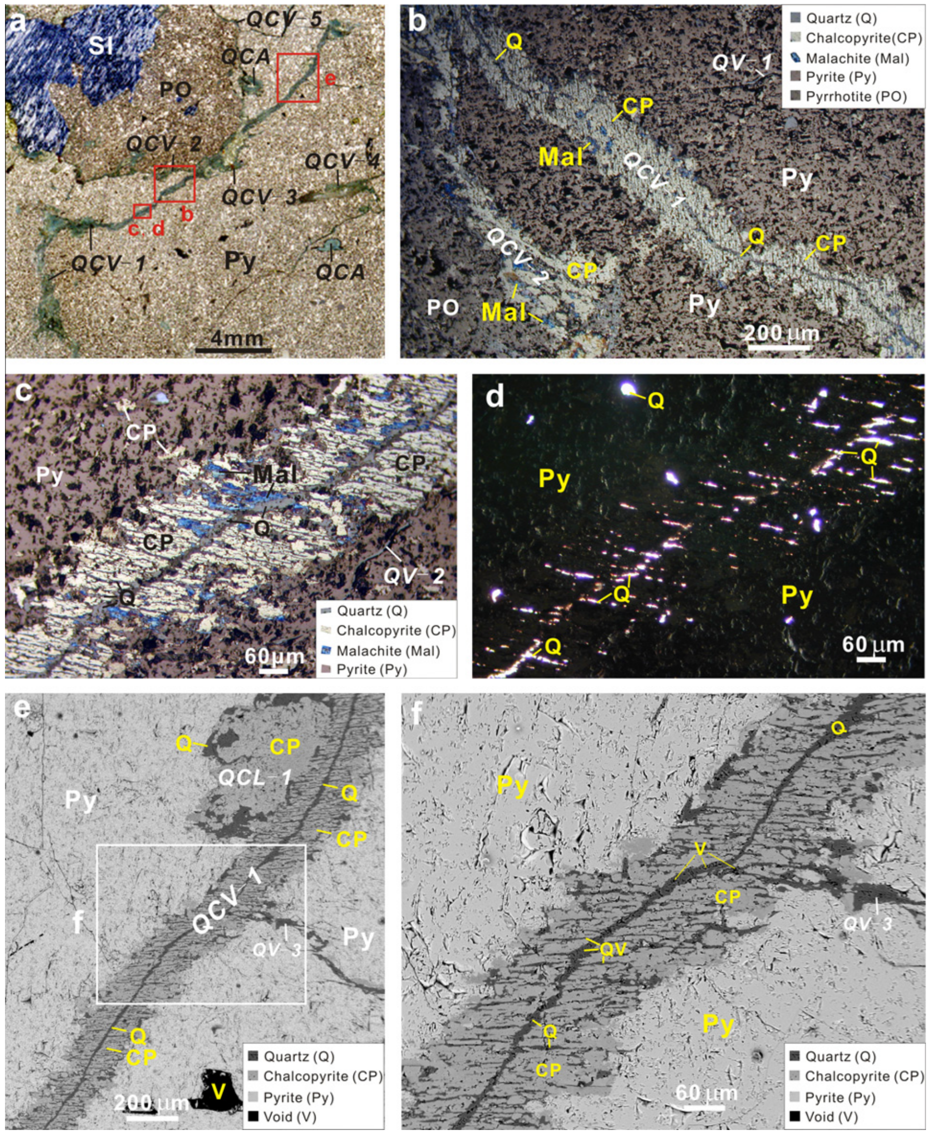

Fig. 3. (a) Scanning image, (b and c) reflecting microscopic images, (d) polarized microscopic images, (e and f) SEM images showing the occurrence and geometry of comb microfractures and their host quartz–chalcopyrite veins (QCV) for the ore specimen HS02 in a thin section from the Hongshan porphyry Cu deposit. The white rectangles in image a show the locations of image b–e, and the white rectangle in image e shows the location of image f. The bright spots and strips in image d show quartz under partial extinction conditions. QCA: quartz–chalcopyrite aggregate; QCV-1, 2, 3 and 4: quartz chalcopyrite vein 1, 2, 3 and 4, respectively; QV-1, 2 and 3: quartz veinlet 1, 2 and 3, respectively.

quartz–sulfide veinlets most likely belong to the late Cretaceous porphyry Cu mineralization system in the Hongshan area.

Quartz–chalcopyrite veinlets are present in pyrite (such as QCV-1, 3 and 5 in Fig. 3a) and along contacts between the composite pyrrhotite–sphalerite inclusions and pyrite (such as QCV-2 and 4) in the shape of fine, irregular curved lines with an approximate width of <1 mm and lengths not exceeding 4 cm. They are characterized by the development of comb-textured microfractures of tooth-shaped quartz veinlets that dismember chalcopyrite fragments (Fig. 3a).

The most typical comb microfractures are in quartz–chalcopyrite vein 1 (QCV-1). This 2.5-cm-long and 0.1–1.1-mm-wide "ʃ"-shaped consists of chalcopyrite (~85 vol.%) and quartz (~15 vol.%) with few >6 μm irregular open cavities (Fig. 3a and f). Comb microfractures in comb- shaped quartz veinlets are well developed in the quartz–chalcopyrite vein (Figs. 3c–e) where they form tooth-shaped quartz veinlets. The 5–10 μm wide quartz teeth are connected to the central longitudinal quartz veinlet at the roots. The teeth quartz veinlets grow into the chalcopyrite, and dismember chalcopyrite grains into fragments (Figs. 3c–f). The width of the chalcopyrite fragments and the distance between two adjacent quartz teeth ranges from 10 μm to 30 μm. Quartz in the comb-like quartz veinlets is <10 μm and microcrystalline or cryptocrystalline (Fig. 3d). Most of the quartz teeth and chalcopyrite pieces grow perpendicular to the central longitudinal quartz veinlets and their host quartz–chalcopyrite veins, while others grow at an angle of more than 60° to the central longitudinal quartz veinlet. Most of the quartz teeth cut through the chalcopyrite to the boundary of the quartz–chalcopyrite vein, and a few of them extended into pyrite in the walls, such as the QV-2 in image c and QV-3 in image d (Figs. 3c, e and f). The quartz teeth and tooth-shaped microfractures are typical textures of tensional hydrofractures (Hubbert and Willis, 1959; Xu et al., 2000, 2001, 2004). Aggregates of <2 mm quartz–chalcopyrite, contain quartz along vein margins and the quartz "teeth" are inserted into chalcopyrite and these also are typical fillings within tensional hydrofractures.

4. Formation mechanism for comb microfractures and their metallogenic significance

Because comb microfractures are restricted within the enclosed quartz–chalcopyrite veinlets, this indicates that microfractures are exclusively related to the quartz–chalcopyrite veins and are not caused by regional tectonic deformation. A great amount of chalcopyrite (>80 vol.%) and low abundance of open cavities or voids (potential agents of aqueous fluid, <5 vol.%) both in the enclosed quartz–chalcopyrite veinlets and in the aggregates indicates that they were most likely crystallized and solidified from a hydrous chalcopyrite–silica melt rather than by hydrothermal solution, similar to quartz and sulfide minerals in vein dikes and to open-space veins at Henderson porphyry Mo deposit (Carten et al., 1988). This is consistent with the occurrence of sulfide melt inclusions in quartz veins in some porphyry copper deposits (Candela, 1997; Keith et al., 1997; Halter et al., 2002, 2005; Core et al., 2006).

Because the chalcopyrite fragments were dismembered by quartz teeth that are rooted in the central quartz vein, hydrofracturing of chalcopyrite was therefore most likely induced by explosion and instant injection of silica melt from the center towards the outside. Pressure that build up within the silica melt and produce comb quartz veinlets would most likely have been related to crystallization and solidification of the confined chalcopyrite–silica melt instead of being related to feeding pressure. Feeding pressure, such as the buoyancy force (e.g., Spence and Turcotte, 1990; Lister and Kerr, 1991; Clemens and Mawer, 1992; Rubin, 1995) and magma driving pressure (Baer and Reches, 1991; Hogan et al., 1998), always creates and propagates fractures at the tips of liquid-filled veins. Moreover, the molar volume of quartz mineral is about 22.7 cm^3/mol (Ackermann and Sorrell, 1974) and less than that of silica melt, which is about 27.3 cm^3/mol (Brfickner, 1970; Courtial and Dingwell, 1999; Rabukhin, 1999), implying that crystallization of quartz from silica melt involves volume contraction with a ratio of about 16.8% and this is consistent with the ratio of the irregular voids hosting quartz in the comb-like quartz veinlet in QCV-1. The volumetric pressures forming the comb microfractures in the quartz–chalcopyrite veins were most likely related to crystallization of chalcopyrite mineral from chalcopyrite melt, although the molar volume of chalcopyrite melt is still unknown.

Textural evidence, therefore, indicates that the silica melts formed the central quartz veinlets were at high pressure and the implications of this are outlined below.

Irregular inlays of chalcopyrite along pyrite margins at the borders of the quartz–chalcopyrite veins (Fig. 3f) indicate that the formation of chalcopyrite most likely involved volume expansion, and therefore the type of pressure driving the silica melt that broke the chalcopyrite was most likely volumetric pressure. Chalcopyrite first crystallized from chalcopyrite–silica melt due to volume expansion—similar to freezing water trapped within pores and cracks (Hall et al., 2002; Hale and Shakoor, 2003). The mechanism is also similar to crystallization of water-saturated granitic melt at a depth about 2 km (Burnham and Ohmoto, 1980). Because the bulk modulus of liquid is very large, about 10^{10-11} Pa for melt (Murase and McBirney, 1973), and about 2.32 GPa for water (Carmichael, 1989), a static confined liquid in elastic lithosphere can be regarded as incompressible. Positive volume changes have the potential to generate high pressures capable of breaking rocks (Xu et al., 2001, 2004), and these positive volume changes can also produce vein-filled fractures and explosive breccias associated that are common within or proximal to porphyritic bodies originating from water-saturated magmas (Bryant, 1968; Llambias and Malvicini, 1969; Sharp, 1979; Sillitoe, 1985; Xu et al., 2000), similar to the creation of fractures in ice (Hall et al., 2002; Hale and Shakoor, 2003).

A hypothetical process causing the formation of the comb microfractures is outlined below (Fig. 4) and illustrates a small amount of chalcopyrite–silica melt injected into a partly crystallized or poorly consolidated pyrite vein. As the pyrite margins crys-

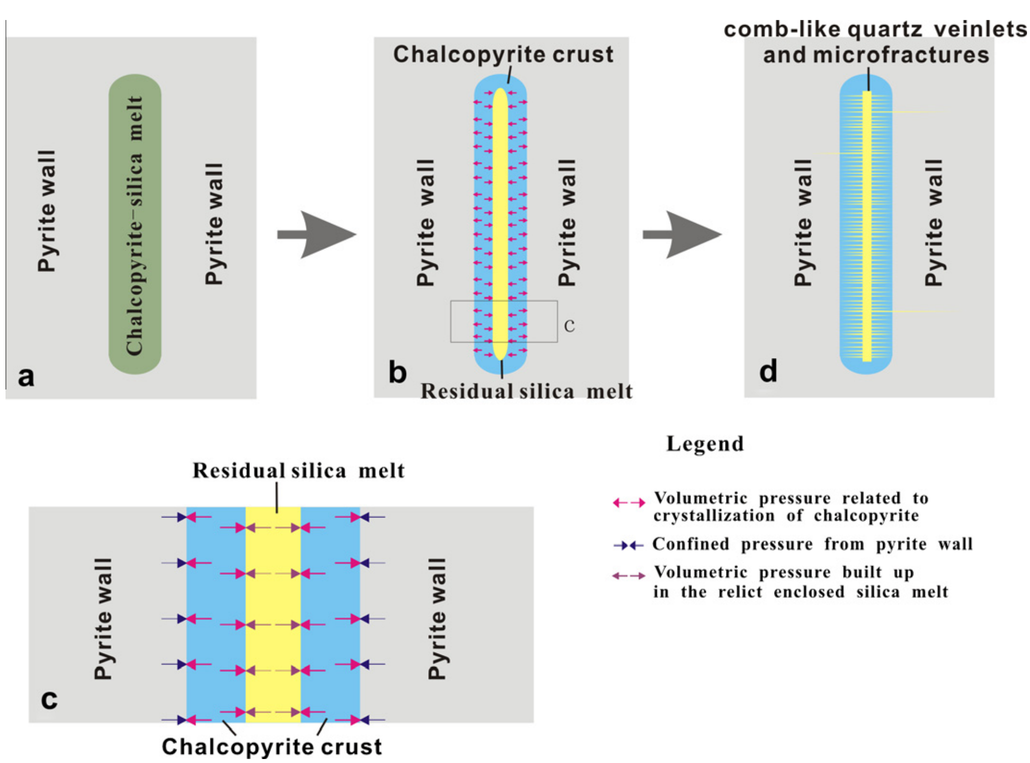

Fig. 4. Formation model for comb microfractures in the quartz–chalcopyrite veins in the Hongshan porphyry Cu deposit, western Yunnan, SW-China.

tallize and became fully consolidated, the thin chalcopyrite–silica melt flow is trapped and enclosed (Fig. 4a). Then, early crystallization of chalcopyrite from this trapped chalcopyrite–silica melt formed a chalcopyrite carapace, resulting in the development of a pipe containing a thick chalcopyrite crust with silica–chalcopyrite melt at the center. During primary crystallization of the trapped chalcopyrite–silica melt, volume expansion related to the crystallization of chalcopyrite melt was balanced by compression from the sulfide wall and by the residual silica–chalcopyrite melt (Fig. 4b). Continued crystallization of chalcopyrite mineral and the resulting volume expansion; however, caused a buildup of pressure within the silica–chalcopyrite melt (Fig. 4c). Upon complete crystallization of the chalcopyrite melt, the pressure in the silica melt was higher than the tensile strength of the surrounding chalcopyrite crust and created tensile fractures perpendicular to the pipe (e.g., Hubbert and Willis, 1959; Atkinson, 1984; Xu et al., 2004). Silica melt was then injected into these microfractures to form comb quartz veinlets and comb microfractures (Fig. 4d). In some cases, silica melt broke through developing microcracks along the chalcopyrite–pyrite contact to form quartz veinlets at the interface, and therefore some silica melt was expelled out into the original enclosing space within the emerging veinlet volume. This process is similar to pore water expulsion during freezing in an open system (e.g., Taber, 1930; Arvidson and Morgenstern, 1977; Chen et al., 1980) and the expulsion of fluids from K-metasomatic systems (Xu et al., 2004).

This mechanism operated on quartz–chalcopyrite aggregates as well. Early crystallization of chalcopyrite most likely drove silica melt aside and also increased the volumetric pressure in residual silica melt enough to break the chalcopyrite.

5. Origin of zonal mineralization in hypogene porphyry copper deposits

5.1. Volume change of mineralization systems

Evidence of volume expansion related to crystallization of chalcopyrite mineral from melt is common in most porphyry copper deposits. Comb microfractures, dendritic and swollen chalcopyrite veins, and compaction fabrics are examples. Dendritic chalcopyrite veinlets are propagated upward at the tip of the fractures on chalcopyrite grains (Fig. 5a) and are related to hydrofracturing of the chalcopyrite melt (Cook and Gordon, 1964; Pollard, 1977; Xu

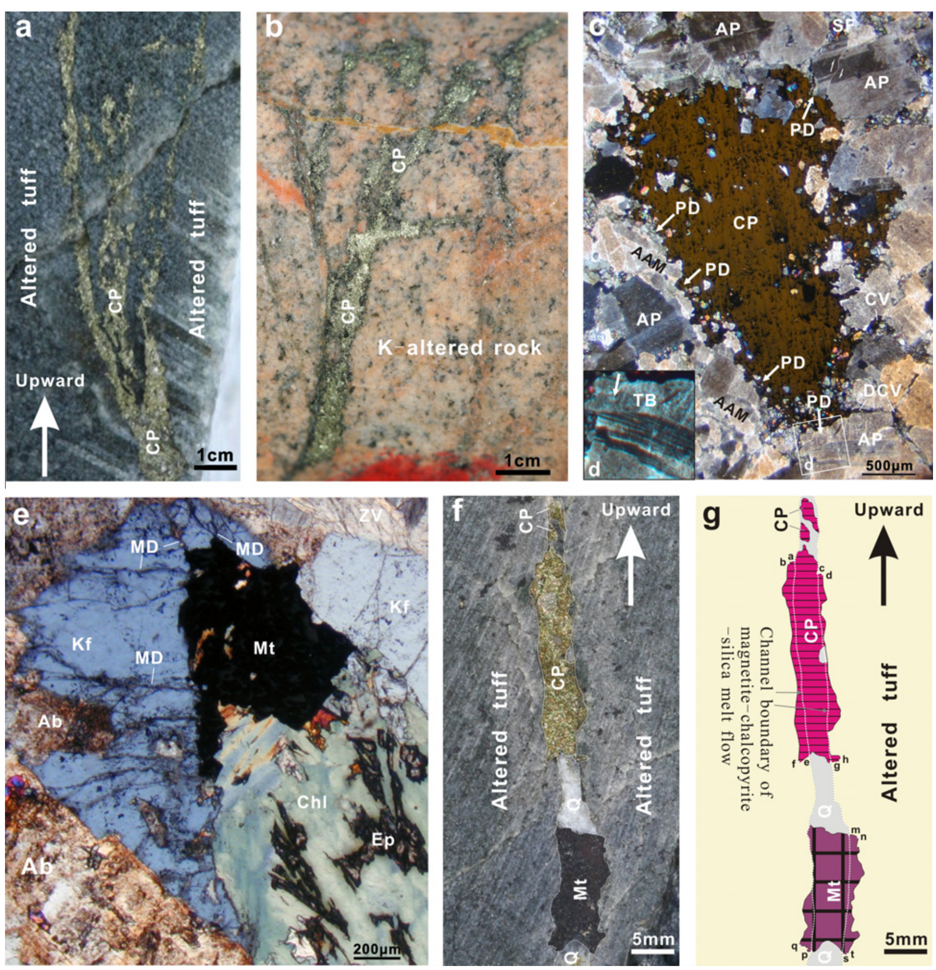

Fig. 5. Photographs and one sketch showing dendritic chalcopyrite and magnetite veinlet, pushing structures and swollen vein. (a) Dendritic chalcopyrite veinlet in altered tuff. (b) Dendritic chalcopyrite veinlet in K-altered rock. (c) Pushing structures (e.g., twin bending, crystal arrangement and intragranular shear fracture in matrix and phenocryst) associated with disseminated chalcopyrite lump embedded in albite matrix and phenocryst in ore-bearing albite porphyry. (d) Local enlargement of twin bending structure in image c. (e) Dendritic magnetite veinlets rooted on an enclosed magnetite crystal in K-altered albite porphyry. (f) Quartz–magnetite–chalcopyrite vein in altered tuff, (g) sketch of image b with suggested channel boundaries of the liquid flow. The ore specimens for images a and f were collected from the drilling core zk006 at a depth of about 306 m and zk005 at a depth of 372 m, respectively in the Mengxi porphyry Cu–Mo deposit, east Junggar, which is characterized by abundant sulfide veins and veinlets in wall rocks and related to the granitic porphyry dikes (Qu et al., 2009). The ore specimens for images b and e were collected from K-altered zone, and that for image c from an ore-bearing albite porphyry dike intruded in granite, in the Hersai porphyry copper deposit, east Junggar. AAM: arranged albite matrix, AP: albite phenocryst, CP: chalcopyrite, CV: chalcopyrite vein, MD: magnetite dendrite, PD: pressing direction, SF: shear fracture, TB: twin bending.

et al., 2004; Xu, 2009). Dendritic chalcopyrite veinlets in altered wall-rocks are commonly isolated (Fig. 5b), indicating that the pressure that created the fractures and the chalcopyrite melt movement was not continuous. Dendritic chalcopyrite veinlets also grow outwards upon some chalcopyrite aggregates that are embedded in the matrix of the host porphyry (Fig. 5c). Volumetric pressure may produce pressure-related deformed structures, such as the outwardly bending of crystallographic twins, parallel arrangement of matrix minerals, and sliding fractures (Fig. 5c and d) on phenocrysts and matrix crystals within the host porphyry. Development of dendritic magnetite veinlets that are rooted on an enclosed magnetite crystal (such as that showed in Fig. 5e) in K-altered albite porphyry indicate that crystallization of magnetite mineral from melt possibly involved volume expansion as well.

The volume expansion ratio of chalcopyrite mineral to melt can be roughly estimated from a massive chalcopyrite vein. The contiguous chalcopyrite in ore veins is commonly wider than the adjacent quartz (Fig. 5f), as that shown by line ab, cd, ef and gh in Fig. 4g. These steps in the chalcopyrite fabric clearly show lateral volume expansion, which was induced by the crystallization of chalcopyrite, because hydrofracturing planes ordinarily should be relatively straight. The thickness of the chalcopyrite melt flow that formed chalcopyrite in the center of the quartz–magnetite–chalcopyrite vein in Fig. 5f and g was most likely equal to the width of the quartz grain on either side. This implies that the volume expansion ratio of chalcopyrite mineral to melt was about 19 vol.%, which is larger than the volume contraction ratio of quartz liquid to mineral. Similarly, it is roughly estimated that the volume expansion ratio of magnetite mineral to melt was about 20 vol.%.

K-metasomatism is one of the most extensive alteration types in porphyry systems and formed at temperatures between 450 °C and 700 °C in porphyry systems (e.g., Fournier, 1967a; Nielsen, 1968; Lowell and Guilbert, 1970; Rose, 1970; Titley, 1982; Seedorff et al., 2005; Cathles and Shannon, 2007) and K-metasomatism also involves a volume increase (Xu et al., 2004). The volume expansion coefficient of molecular lattices for the replacement of albite and anorthite by orthoclase can be roughly estimated using the following metasomatic reactions (Orville, 1963; Deng, 1986; Collins, 1996):

$$\underset{\text{(Albite)}}{NaAlSi_3O_8} + K^+ = \underset{\text{(Orthoclase)}}{KAlSi_3O_8} + Na^+ \quad (1)$$

$$\underset{\text{(Anorthite)}}{CaAl_2Si_2O_8} + 4SiO_2 + 2K^+ = \underset{\text{(Orthoclase)}}{2KAlSi_3O_8} + Ca^{2+} \quad (2)$$

The volume expansion rate of a monomolecular lattice is about 8.6 vol.% for orthoclase replacing albite and13.4 vol.% for orthoclase replacing anorthite and quartz (Xu et al., 2004).

In summary, crystallization of chalcopyrite and magnetite and the formation of metasomatic orthoclase within the mineralization system of porphyry copper deposits involve volume expansion, which then has the potential to increase volumetric pressure enough to create fractures and to open up the system to fluid flow.

5.2. Features and origin of porphyry magma for porphyry copper deposits

The close spatial and temporal relation among hydrothermal deposits and magmatic intrusions, the regular zoning of alternation minerals, the coexistence of sulfide and silicate melt inclusions that contain vapor-rich and hypersaline fluid inclusions formed at near magmatic temperatures, and the distinct lead and sulfur isotope data for porphyry copper deposits suggest that the ore-forming fluids were magmatic (e.g., Ulrich et al., 1999; Halter et al., 2002; Holliday et al., 2002; Harris and Golding, 2002; Harris et al., 2003; Redmond et al., 2004; Core et al., 2006), and that these fluid exsolved and travelled outward from a porphyry magma (e.g., Hedenquist and Lowenstern, 1994; Guillou-Frottier and Burov, 2003; Heinrich et al., 2004; Williams-Jones and Heinrich, 2005). Both porphyry copper deposits and their host porphyritic stocks and plutons are likely the twinborn products of ore-forming fluid-rich porphyry magmas.

Recent research (Xu et al., 2009b) suggests that many porphyry bodies were shallow intrusions of mixed melts that contained phenocrysts and glomeroporphyritic aggregates, which were formed by fractional crystallization and accumulation in a deeper transitional magma chamber.

Fractional crystallization, accumulation and concentration of silicate minerals from melt in a magma chamber are enrichment process for ore elements such as Au, Cu and Mo (e.g., Candela and Holland, 1986; Richards, 2003; Mustard et al., 2006). Incompatible ore elements, such as Mo, sulfide melt, aqueous liquid, and vapor are directly concentrated in magma during silicate mineral crystallization (e.g., Candela and Holland, 1986; Hedenquist and Lowenstern, 1994). On the other hand, a compatible element like Cu may be concentrated in magma by partitioning of sulfide liquid and sulfate–chloride-bearing fluid (e.g., Candela, 1997; Halter et al., 2002; Harris et al., 2003; Williams-Jones and Heinrich, 2005). Pulsed input of new melt into a magma chamber while crystallized silicate minerals are removed from the melt will gradually concentrate base metals, producing ore-forming melts in small amounts (Lowenstern, 1994; Ulrich et al., 1999). Ore-bearing porphyry magmas formed when the residual ore-forming melts, containing some phenocrysts and glomeroporphyritic aggregates, were emplaced at a shallow crustal level.

5.3. Crystallization of ore-bearing porphyry magma and mineralization zoning

On the basis of features of ore-forming porphyry magmas and on the basis of known volume expansion, related to K-metasomatism and crystallization of magnetite and chalcopyrite, it is convenient to apply a modified "orthomagmatic" genetic model to account for the mechanisms responsible for zoning of mineralization within porphyry copper deposits, after Burnham (1967), Nielsen (1968), Philips (1973), and Whitney (1975, 1984).

Application of this modified hypothetical "orthomagmatic" genetic model suggests that crystallization of ore-bearing porphyry magma and the formation of porphyry copper deposits would have undergone three main stages as outlined below (Fig. 6):

In the first stage (Stage I) (Fig. 6a), early crystallization of shallowly emplaced, ore-bearing porphyry magma along the walls and roof of the magma chamber produced a solid carapace around the liquid intrusion (Nielsen, 1968; Edwards and Atkinson, 1986). Hydrous fluids are then exsolved from the magma and are concentrated in the apical region of the intrusion beneath the carapace (Whitney, 1975; Burnham, 1979). As internal vapor pressure increases, which is partly induced by retrograde boiling (Philips, 1973), rising fluid pressures exceed the lithostatic pressure and the tensile strength of the crystalline carapace, the rocks and host rock therefore fracture, permitting rapid escape of hydrous fluids into the newly created open spaces above the carapace and magma chamber and newly forming vein system (e.g., Hubbert and Willis, 1959; Atkinson, 1984; Xu et al., 2004). The initially exsolved hydrous fluids are then enriched in aqueous vapor containing sulfide melts and many other components (e.g., Candela and Holland, 1986; Manning and Pichavant, 1988; Candela, 1989; Cline and Bodnar, 1991; Heinrich, 1990; Halter et al., 2005). Zoning results from the precipitation and replacement of minerals along fracture within the outwardly expanding vein system. Mesothermal orthoclase and biotite form near the magma intrusion, and are followed by quartz and sericitic alteration. Propylitic alteration in the wall

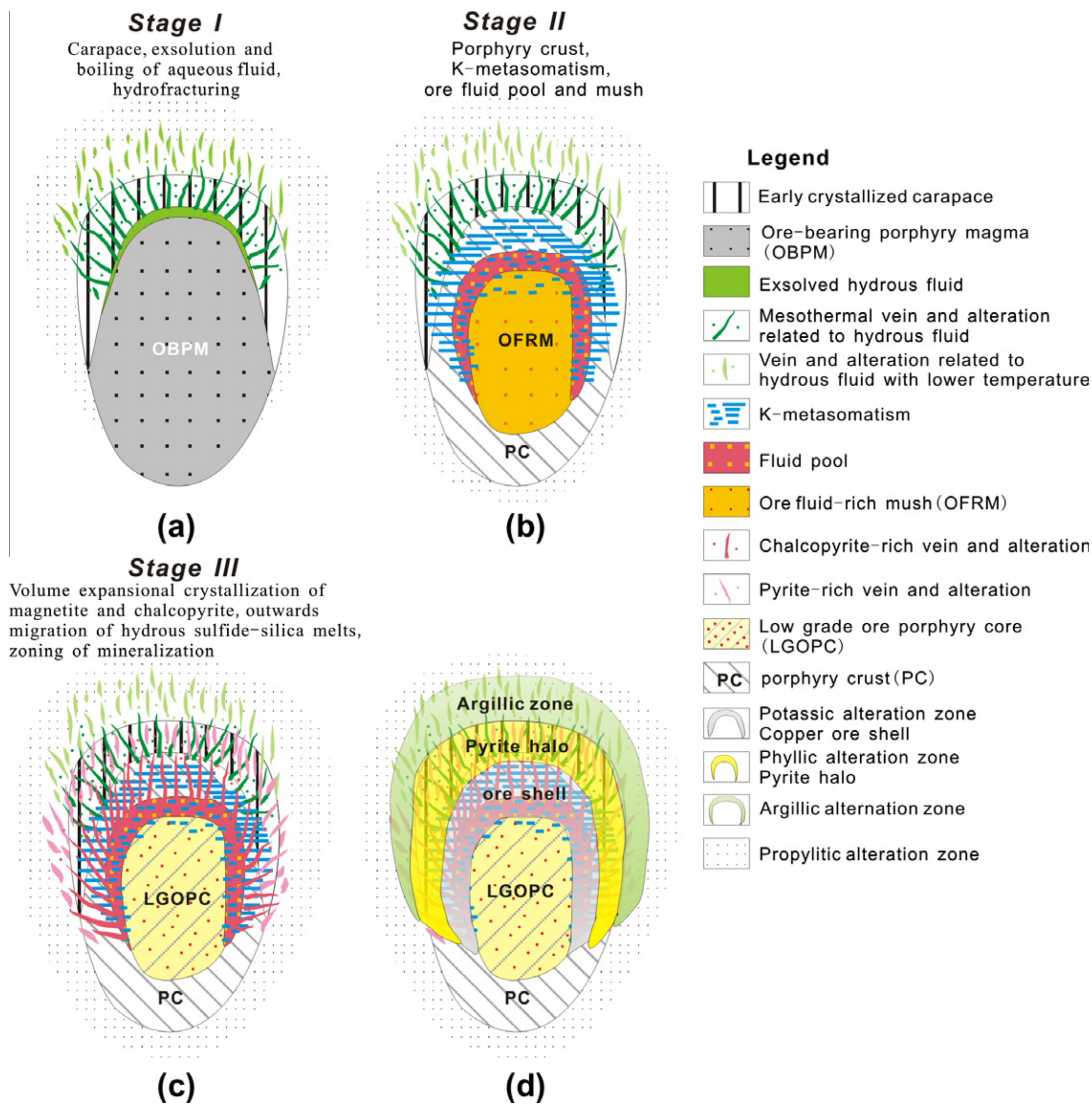

Fig. 6. Genetic model for zonal mineralization of hypogene porphyry copper deposits.

rocks occurs at relatively cooler temperatures. Early crystallization of chalcopyrite mineral from melt within veins had the potential to precipitate chalcopyrite mainly in the crystalline carapace.

The second stage involves continued crystallization that produces a porphyritic crust and increases the volume of ore-forming fluid that contains sulfide melt within the central crystal-melt core (Fig. 6b). The ore-forming fluids are possibly brines enriched in potassium. In this stage (Stage II), intensive K-metasomatism in the upper crust close to the magma and the carapace produces an orthoclase shell. This is where early fractures and veins are replaced and less active elements (e.g., Mg, Fe and Cu) and minerals (such as chalcopyrite) are trapped. Meanwhile, ore-rich fluids separate out and are concentrated at the upper contacts between the porphyry crust and the mush core to form a saddle-shaped, ore-rich fluid pool. In addition, space is conserved due to volume expansion by K-metasomatism that is matched by volume contraction of crystallization and solidification of the porphyry crust during the crystallizing magmas. K-metasomatism occurs in the mush core as well, and some plagioclase phenocrysts that form in the pre-emplaced magma chamber may be replaced by orthoclase or sericite aggregates.

During the third stage (Stage III), further crystallization of the crystal-melt (mush) core ore-forming fluids are enclosed in pores within the groundmass. These pore fluids develop into alteration within the groundmass and phenocrysts by the growth of orthoclase, sericite, quartz, and locally kaolinite where there were higher numbers of hydrogen ions. When the trapped ore-forming fluids crystallize, sulfide minerals are precipitated and disseminated within the altered core porphyry, forming a low-grade ore core (Figs. 6c and 5d). Volume expansion, due to crystallization of magnetite and chalcopyrite in the pore fluid, increases the pressure sufficient to break the host rocks, allowing fluids to flow into the hydrofractures and producing ore-bearing veinlets and compaction structures (Fig. 5c). When pore fluid is connected by veinlets, some leftover ore-forming fluids may be expelled up and outwards into the fluid pool. This process is similar to pore water expulsion during freezing in an open system (e.g., Taber, 1930; Arvidson and Morgenstern, 1977; Chen et al., 1980).

Both fluid injections from the mushy core and volume expansion that is related to K-metasomatism and crystallization of magnetite and chalcopyrite, increase pressure within the fluid pool. When the volumetric pressure of the fluids exceeded the lithostatic pressure and the tensile strength of the orthoclase shell, hydrofractures and ore-forming fluids veinlets form along the orthoclase shell. Prior volume increase, due to crystallization of magnetite and chalcopyrite in the fluid veinlets, propagates fractures and re-moves leftover fluid from the orthoclase shell by allowing the fluid to flow up and outwards. These hydrofractures seal due to continued crystallization and precipitation, and this "throttling" allowing the pressure of the fluid pool to increase again (Edwards and Atkinson, 1986). This sequence repeats many times. As a result, quantities of chalcopyrite residing in the orthoclase shell form an ore shell and pyrite and quartz are precipitated in a zone close to the ore shell forming a pyrite halo. Aqueous fluid moves to the outer zone and causes forms an argillic alternation zone due to superposed hydrogen metasomatism (Fig. 6d).

6. Conclusion

Comb quartz veinlets are well developed on quartz–chalcopyrite in vein in the Hongshan porphyry Cu deposit of Zhongdian County in eastern Tibet. Teeth-shaped quartz is perpendicularly rooted in the central parts of the quartz veinlet, and dismembers chalcopyrite in the veins and veinlets. These tooth-shaped microfractures, filled by microcrystalline or cryptocrystalline quartz, are typical tensional hydrofractures. The formation of these comb microfractures is related to volume expansion that was induced by crystallization of chalcopyrite mineral from chalcopyrite melt and to the subsequent increase in volumetric pressure in the confined silica melt. Volumetric pressures caused the expulsion of some silica melt into pyrite in the adjacent wall rock. The formation mechanism that developed the comb microfractures, including volume expansion induced by crystallization, increase in volumetric pressure, hydrofracturing and fluid expulsion, is hypothesized as the main process for zoning in porphyry copper deposits.

Textures typical of volumetric pressure such as dendritic and deformed veins were the common structures induced by related to crystallization of chalcopyrite and magnetite and K-metasomatism in porphyry copper deposits. The volume expansion ratio of chalcopyrite mineral to melt and that of magnetite mineral to melt were about 19 vol.% and 20 vol.%, respectively. The volume expansion rate of a monomolecular lattice is more than 8 vol.% for orthoclase replacing plagioclase.

Based on the volume variety in crystallization, K-metasomatism and solidification processes of ore-forming magmas, we propose a new, modified "orthomagmatic" genetic model for zoning of minerals in porphyry copper deposits. It is suggested that porphyry copper deposits are associated products of crystallization and solidification of ore-bearing magma intrusions. Zoning of mineralization, from disseminated ore core and ore shell to outer pyrite halo, is primarily related to the regular migration and distribution of ore-forming fluids and involves a series of substantial processes, such as the concentration of ore-forming fluids in the mush core, exsolving and migration of ore-forming fluids containing sulfide melts from the mush core to form the saddle-shaped ore-forming fluids pool, K-metasomatism and formation of K-feldspar shell and pressure building in the enclosed fluid pool, and hydrofractures and injection and migration of ore-forming fluids into the orthoclase shell along hydrofractures. The continued hydrofractures are due to prior crystallization of magnetite and chalcopyrite from the ore-forming fluids that is concentrated in the orthoclase shell and is associated with expulsion of residual fluid that is driven by high volumetric pressure. This new model clearly shows origin of the spatial distribution of alteration and mineralization with respect to a cylindrical magmatic stock.

Acknowledgements

This research was supported by the NSFC (Grant Number 41072060), the CAS Knowledge Innovation Project (Grant Numbers kzcx-ew-ly03 and kzcx2-yw-107-2) and the National 305 project (Grant Numbers 2011BAB06B03-3 and 2006BAB07B01-03). We would like to express our gratitude to Changchun Yang, Xin-Ping Cai and Jie Wang for valuable discussions. This paper was significantly improved by the thorough and incisive review of Wenjiao Xiao, Juhn G. Liou and Bor-ming Jahn, and English editing by Stephen G. Peters.

References

Ackermann, R.J., Sorrell, C.A., 1974. Thermal expansion and the high-low transformation in quartz. I. High-temperature X-ray studies. Journal of Applied Crystallography 7, 461–467.
Arvidson, W.D., Morgenstern, N.R., 1977. Water flow induced by soil freezing. Canadian Geotechnical Journal 14, 237–245.
Atkinson, B.K., 1984. Sub critical crack growth in geological materials. Journal of Geophysical Research 89B, 4077–4114.
Baer, G., Reches, Z., 1991. Mechanics of emplacement and tectonic implications of the Ramon dike systems, Israel. Journal of Geophysical Research 96, 11895–11910.
Barnes, H.L., 1962. Mechanisms of mineral zoning. Economic Geology 57, 30–37.
Beane, R.E., Bodnar, R.J., 1995. Hydrothermal fluids and hydrothermal alteration in porphyry copper deposits. In: Pierce, F.W., Bohm, J.G. (Eds.), Porphyry Copper Deposits of the American Cordillera: Arizona Geological Society Digest 20, Tucson, pp. 83–93.
Brfickner, R., 1970. Properties and structure of vitreous silica. Journal of Non-Crystalline Solids 5, 123–175.
Bryant, D.G., 1968. Intrusive breccias associated with ore, Warren (Bisbee) Mining District, Arizona. Economic Geology 63, 1–12.
Burnham, C.W., 1967. Hydrothermal fluids at the magmatic stage. In: Barnes, H.L. (Ed.), Geochemistry of Hydrothermal Ore Deposits. Holt, Rinehart and Winston, Inc., New York, pp. 166–235.
Burnham, C.W., 1979. The importance of volatile constituents. In: Yoder, H.S. Jr., (Eds.), The Evolution of the Igneous Rocks. Princeton University Press, Princeton, NJ, pp. 439–482.
Burnham, C.W., Ohmoto, H., 1980. Late-stage processes in felsic magmatism. Mining Geology Special Issue 8, 1–11.
Candela, P.A., 1989. Calculation of magmatic fluid contributions to porphyry-type ore systems: predicting fluid inclusion chemistries. Geochemical Journal 23, 295–305.
Candela, P.A., 1992. Controls on ore metal ratios in granite-related ore systems: an experimental and computational approach. Transactions of the Royal Society of Edinburgh—Earth Sciences 83, 317–326.
Candela, P.A., 1997. A review of shallow, ore-related granites: textures, volatiles, and ore metals. Journal of Petrology 38, 1619–1633.
Candela, P.A., Holland, H.D., 1986. A mass transfer model for copper and molybdenum in magmatic hydrothermal systems. The origin of porphyry-type ore deposits. Economic Geology 81, 1–19.
Carmichael, R.S., 1989. Practical Handbook of Physical Properties of Rocks and Minerals. CRC Press, Boston, p. 741.
Carten, R.B., Geraghty, E.P., Walker, B.M., Shannon, J.R., 1988. Cyclic development of igneous features and their relationship to high-temperature hydrothermal features in the Henderson porphyry molybdenum deposit, Colorado. Economic Geology 83, 266–296.
Cathles, L.M., Shannon, R., 2007. How potassium silicate alteration suggests the formation of porphyry ore deposits begins with the nearly explosive but barren expulsion of large volumes of magmatic water. Earth and Planetary Science Letters 262, 92–108.
Chen, X., Jiang, P., Wang, Y., 1980. Pore water pressure of saturated gravel during freezing. Journal of Glaciology and Cryopedolgy 2 (4), 33–37 (in Chinese).
Chung, S.L., Lo, C.H., Lee, T.Y., Zhang, Y., Xie, X., Li, X., Wang, K.L., Wang, P.L., 1998. Diachronous uplift of the Tibetan plateau starting 40 Ma ago. Nature 394, 769–773.
Clemens, J.D., Mawer, C.K., 1992. Granitic magma transport by fracture propagation. Tectonophysics 204, 339–360.
Cline, J.S., Bodnar, R.J., 1991. Can economic porphyry copper mineralization be generated by a typical calc-alkaline melt? Journal of Geophysical Research 96, 8113–8126.
Collins, L.G., 1996. The Metasomatic origin of the Cooma complex in southeastern Australia. Theophrastus Contributions to Advanced Studies in Geology 1, 105–112.
Cook, J., Gordon, J.E., 1964. A mechanism for the control of crack propagation in all brittle systems. Proceedings of the Royal Society of London (Series A) 282, 508–520.
Cooke, D.R., Hollings, P., Walsh, J.L., 2005. Giant porphyry deposits: characteristics, distribution, and tectonic controls. Economic Geology 100, 801–818.
Core, D.P., Kesler, S.E., Essene, E.J., 2006. Unusually Cu-rich magmas associated with giant porphyry copper deposits: evidence from Bingham, Utah. Geology 34, 41–44.
Corn, R.M., 1975. Alteration-mineralization zoning, Red Mountain, Arizona. Economic Geology 70, 1437–1447.
Courtial, P., Dingwell, D.B., 1999. Densities of melts in the CaO–MgO–Al_2O_3–SiO_2 system. American Mineralogist 84, 465–476.

Deng, J., 1986. Phase Equilibrium and Origin of Petrology. China University of Geosciences Press, Wuhan, p. 32 (in Chinese).
Edwards, R., Atkinson, K., 1986. Ore Deposit Geology. Chapman and Hall, London, p. 466.
Fournier, R.O., 1967a. The porphyry copper deposit exposed in the Liberty open-pit mine near Ely, Nevada. Part I. Syngenetic formation. Economic Geology 62, 57–81.
Fournier, R.O., 1967b. The porphyry copper deposit exposed in the Liberty open-pit mine near Ely, Nevada. Part II. The formation of hydrothermal alteration zones. Economic Geology 62, 207–227.
Guillou-Frottier, L., Burov, E., 2003. The development and fracturing of plutonic apexes: implications for porphyry ore deposits. Earth and Planetary Science Letters 214, 341–356.
Guo, Z.F., Hertogen, J., Liu, J.Q., Pasteels, P., Boven, A., Punzalan, L., He, H.Y., Luo, X.J., Zhang, W.H., 2005. Potassic magmatism in western Sichuan and Yunnan Provinces, SE Tibet, China: petrological and geochemical constraints on petrogenesis. Journal of Petrology 46, 33–78.
Hale, P.A., Shakoor, A., 2003. A laboratory investigation of the effects of cyclic heating and cooling, wetting and drying, and freezing and thawing on the compressive strength of selected sandstones. Environmental and Engineering Geoscience 9, 117–130.
Hall, K., Thorn, C.E., Matsuoka, N., Prick, A., 2002. Weathering in cold regions: some thoughts and perspectives. Progress in Physical Geography 26, 577–603.
Halter, W.E., Pettke, T., Heinrich, C.A., 2002. The origin of Cu/Au ratios in porphyry-type ore deposits. Science 296, 1844–1846.
Halter, W.E., Heinrich, C.A., Pettke, T., 2005. Magma evolution and the formation of porphyry Cu–Au ore fluids: evidence from silicate and sulfide melt inclusions. Mineralium Deposita 39, 845–863.
Harris, A.C., Golding, S.D., 2002. New evidence of magmatic-fluid-related phyllic alteration: implications for the genesis of porphyry Cu deposits. Geology 30, 335–338.
Harris, A.C., Kamenetsky, V.S., White, N.C., Achterbergh, E.V., Ryan, C.G., 2003. Melt inclusions in veins: linking magmas and porphyry Cu deposits. Science 302, 2109–2111.
Hedenquist, J.W., Lowenstern, J.B., 1994. The role of magmas in the formation of hydrothermal ore deposits. Nature 370, 519–527.
Heinrich, C.A., 1990. The chemistry of hydrothermal tin (-tungsten) ore deposition. Economic Geology 85, 457–481.
Heinrich, C.A., Driesner, T., Stefánsson, A., Seward, T.M., 2004. Magmatic vapor contraction and the transport of gold from the porphyry environment to epithermal ore deposits. Geology 32, 761–764.
Hemley, J.J., Jones, W.R., 1964. Chemical aspects of hydrothermal alteration with emphasis on hydrogen metasomatism. Economic Geology 59, 538–569.
Hemley, J.J., Cygan, G.L., Fein, J.B., Robinson, G.R., d'Angelo, W.M., 1992a. Hydrothermal ore-forming processes in the light of studies in rock-buffered systems – I. Iron–copper–zinc–lead sulfide solubility relations. Economic Geology 87, 1–22.
Hemley, J.J., Cygan, G.L., Fein, J.B., Robinson, G.R., d'Angelo, W.M., 1992b. Hydrothermal ore-forming processes in the light of studies in rock-buffered systems—II. Some general geologic applications. Economic Geology 87, 23–43.
Hogan, J.P., Price, J.D., Gilbert, M.C., 1998. Magma traps and driving pressure: consequences for pluton shape and emplacement in an extensional regime. Journal of Structural Geology 20, 1155–1168.
Holliday, J.R., Wilson, A.J., Blevin, P.L., Tedder, I.J., Dunham, P.D., Pitzner, M., 2002. Porphyry gold–copper mineralisation in the Cadia district, eastern Lachlan Fold Belt, New South Wales, and its relationship to shoshonitic magmatism. Mineralium Deposita 37, 100–116.
Hou, Z., Ma, H., Khin, Z., Zhang, Y., Wang, M., Wang, Z., Pan, G., Tang, R., 2003. The Himalayan Yulong porphyry Cu belt: product of large-scale strike-slip faulting in eastern Tibet. Economic Geology 18, 125–145.
Hou, Z.Q., Zaw, K., Pan, G.T., Mo, X.X., Xu, Q., Hu, Y.Z., Li, X.Z., 2007. Sanjiang Tethyan metallogenesis in S.W. China: Tectonic setting, metallogenic epochs and deposit types. Ore Geology Reviews 31, 48–87.
Hu, R., Bi, X., Shao, S., Turner, G., Burnard, P.G., 1997. Study on helium isotope composition of Cu deposit in Machangjing, Yunnan, China. Chinese Science Bulletin 42, 1542–1545 (in Chinese).
Hubbert, M.K., Willis, D.G., 1959. Mechanics of hydraulic fracturing. Journal of Petroleum Technology 9, 153–168.
Keith, J.D., Whitney, J.A., Hattori, K., Ballantyne, G.H., Christiansen, E.H., Barr, D.L., Cannan, T.M., Hook, C.J., 1997. The role of magmatic sulphides and mafic alkaline magmas in the Bingham and Tintic mining districts, Utah. Journal of Petrology 38, 1679–1690.
Lister, J.R., Kerr, R.C., 1991. Fluid-mechanical models of crack propagation and their application to magma transport in dikes. Journal of Geophysical Research 96B, 10049–10077.
Llambias, E.J., Malvicini, L., 1969. Geology and genesis of the Bi–Cu mineralized breccia-pipe, San Francisco de los Andes, San Juan, Argentina. Economic Geology 64, 271–286.
Lowell, J.D., Guilbert, J.M., 1970. Lateral and vertical alteration-mineralization zoning in porphyry ore deposits. Economic Geology 65, 373–408.
Lowenstern, J.B., 1994. Dissolved volatile concentrations in an ore-forming magma. Geology 22, 893–896.
Manning, D.A.C., Pichavant, M., 1988. Volatiles and their bearing on the behaviour of metals in granitic systems. In: Taylor, R.P., Strong, D.F. (Eds.), Recent Advances in the Geology of Granite-related Mineral Deposits. The Canadian Institute of Mining and Metallurgy, Special Vol. 39, pp. 13–24.
Murase, T., McBirney, A.R., 1973. Properties of some common igneous rocks and their melts at high temperatures. Geological Society of America Bulletin 84, 3563–3592.
Mustard, R., Ulrich, T., Kamenetsky, V.S., Mernagh, T., 2006. Gold and metal enrichment in natural granitic melts during fractional crystallization. Geology 34, 85–88.
Nielsen, R.L., 1968. Hypogene texture and mineral zoning in a copper-bearing granodiorite porphyry stock, SantaRita, New Mexico. Economic Geology 63, 37–50.
Orville, P.M., 1963. Alkali ion exchange between vapor and feldspar phase. American Journal of Sciences 261, 201–237.
Park, C.F., 1955. The zonal theory of ore deposits. In: 50th Anniversary Volume of Economic Geology, pp. 226–248.
Park, C.F., 1957. The problem of vertical zoning. Economic Geology 52, 477–481.
Peng, Z., Watanabe, M., Hoshino, K., Sueoka, S., Yano, T., Nishido, H., 1998. The Machangqing copper–molybdenum deposits, Yunnan, China – an example of Himalayan porphyry-hosted Cu–Mo mineralisation. Mineralogy and Petrology 63, 95–117.
Philips, W.J., 1973. Mechanical effects of retrograde boiling and its probable importance in the formation of some porphyry ore deposits. Transactions of the Canadian Institute of Mining and Metallurgy B82, 90–98.
Pollard, D.D., 1977. Derivation and evaluation of a mechanical model for sheet intrusions. Tectonophysics 19, 233–269.
Qu, X., Xu, X.W., Liang, G.L., Qu, W.J., Du, S.J., Jiang, N., Wu, H.P., Zhang, Y., Xiao, H., Dong, L.H., 2009. Geology and Re-Os age of the Mengxi Cu-Mo deposit and element geochemistry of intrusions in the Qiongheba area and its constraint to tectonic setting of the Qiongheba magmatic arc in eastern Junggar, Xinjiang. Acta Petrologica Sinica 25, 765–776 (in Chinese with English abstract).
Rabukhin, A.I., 1999. Structural interpretation of concentration dependences of glass molar volume in systems $R_20–R'_20–SiO_2$, $RO–R'O–SiO_2$, and $R_20–RO–SiO_2$. Glass and Ceramics 56, 11–12.
Redmond, P.B., Einaudi, M.T., Inan, E.E., Landtwing, M.R., Heinrich, C.A., 2004. Copper deposition by fluid cooling in intrusion-centered systems: new insights from the Bingham porphyry ore deposit, Utah. Geology 32, 217–220.
Richards, J.P., 2003. Tectono-magmatic precursors for porphyry Cu–(Mo–Au) deposit formation. Economic Geology 98, 1515–1533.
Rose, A.W., 1970. Zonal relations of wallrock alteration and sulfide distribution at porphyry copper deposits. Economic Geology 65, 920–936.
Rowins, S.M., 2000. Reduced porphyry copper–gold deposits: a new variation on an old theme. Geology 28, 491–494.
Rubin, A.M., 1995. Propagation of magma-filled cracks. Annual Reviews of Earth and Planetary Science 23, 287–336.
Rui, Z., Huang, C., Qi, G., 1984. Porphyry Copper (Molybdenum) Deposits of China. Geological Publishing House, Beijing, pp. 340–360 (in Chinese).
Seedorff, E., Dilles, J.H., Proffett, J.M., Einaudi, M.T., Zurcher, L., Stavast, W.J.A., Johnson, D.A., Barton, M.D., 2005. Porphyry deposits: characteristics and origin of hypogene features. In: Economic Geology 100th. Anniverary, pp. 251–298.
The Seventh Geological Survey Team of Yunnan Bureau of Geology and Mineral Resource (SGSTYBGMR), 1971. Prospecting Report of the Hongshan Copper Deposit in the Zhongdian Area, Yunnan Province, pp. 1–44.
Sharp, J.E., 1979. Cave Peak, a molybdenum-mineralized breccia pipe complex in Culberson County, Texas. Economic Geology 74, 517–534.
Sillitoe, R.H., 1985. Ore-related breccias in volcano plutonic areas. Economic Geology 80, 1467–1514.
Sillitoe, R.H., 2010. Porphyry copper systems. Economic Geology 105, 3–41.
Spence, D.A., Turcotte, D.L., 1990. Buoyancy-driven magma fracture: a mechanism for ascent through the lithosphere and the emplacement of diamonds. Journal of Geophysical Research B95, 5133–5139.
Taber, S., 1930. The mechanics of frost heaving. Journal of Geology 38, 303–317.
Titley, S.R., 1982. The style and progress of mineralization and alteration in porphyry systems. In: Titley, S.R. (Ed.), Advances in Geology of the Porphyry Copper Deposits, Southwestern North America. University of Arizona Press, Tucson, Arizona, pp. 93–116.
Ulrich, T., Gunther, D., Heinrich, C.A., 1999. Gold concentrations of magmatic brines and the metal budget of porphyry copper deposits. Nature 399, 676–679.
Wang, J.H., Yin, A., Harrison, T.M., Grove, M., Zhang, Y.Q., Xie, G.H., 2001. A tectonic model for Cenozoic igneous activities in the eastern Indo-Asian collision zone. Earth and Planetary Science Letters 188, 123–133.
Whitney, J.A., 1975. Vapour generation in a quartz monzonite magma: a synthetic model with application to porphyry copper deposits. Economic Geology 70, 346–358.
Whitney, J.A., 1984. Volatiles in magmatic systems. In: Whitney, J.A., Henley, R.W., Truesdell, A.H., Barton, P.B. (Eds.), Fluid-Mineral Equilibria in Hydrothermal Systems. Society of Economic Geologists, Reviews in Economic Geology, vol. 1, pp. 155–175.
Williams, T.J., Candela, P.A., Piccoli, P.M., 1995. The partitioning of copper between silicate melts and two-phase aqueous fluids: an experimental investigation at 1 kbar, 800 C, and 0.5 kbar, 850 C. Contributions to Mineralogy and Petrology 121, 388–399.
Williams-Jones, A.E., Heinrich, C.A., 2005. 100th Anniversary special paper: vapor transport of metals and the formation of magmatic-hydrothermal ore deposits. Economic Geology 100, 1287–1312.
Xu, X.W., 2009. Dendritic microfractures. Journal of Structural Geology 31, 1061.
Xu, X.W., Cai, X.P., Qun, D., Wang, J., Liang, G., Zhang, X., Liu, L., 2000. Fluids double-fracturing genetic mechanism and mineralization of gold–copper of the breccia pipe at Qibaoshan in Shandong Province. Science in China (Series D) 43, 113–121.

Xu, X.W., Cai, X.P., Wang, J., Zhang, B.L., Liang, G.H., 2001. Tectonic dynamics of fluids and its advance. Advance in Earth Sciences 16, 324–331 (in Chinese with English abstract).
Xu, X.W., Cai, X.P., Zhang, B.L., Wang, J., 2004. Explosive microfractures induced by K-metasomatism. Journal of Asia Earth Sciences 23, 421–423.
Xu, X.W., Cai, X.P., Qu, W.J., Song, B.C., Zhang, B.L., 2006a. Later Cretaceous granitic porphyritic Cu–Mo mineralization system in the Hongshan Area, Northwestern Yunnan and its significances for tectonics. Acta Geologica Sinica 80, 1422–1433 (in Chinese with English abstract).
Xu, X.W., Cai, X.P., Song, B.C., Zhang, B.L., Ying, H.R., Xiao, Q.B., Wang, J., 2006b. Petrologic, chronological and geochemistry characteristics and formation mechanism of alkaline porphyries in the Beiya gold district, western Yunnan. Acta Petrologica Sinica 22, 631–642 (in Chinese with English abstract).
Xu, X.W., Cai, X.P., Xiao, Q.B., Peters, S.G., 2007a. Porphyry Cu–Au and associated polymetallic Fe–Cu–Au deposits in the Beiya Area, Western Yunnan Province, South China. Ore Geology Reviews 31, 224–226.
Xu, X.W., Cai, X.P., Zhang, B.L., Liang, G.H., Du, S.J., Wang, J., 2007b. Genetic types and framework model of Beiya gold ore district in western Yunnan. Mineral Deposits 26, 249–264 (in Chinese with English abstract).
Xu, X.W., Cai, X.P., Zhong, J.Y., Song, B.C., Peters, S.G., 2007c. Formation of tectonic peperites from alkaline magmas intruded into wet sediments in the Beiya area, western Yunnan, China. Journal of Structural Geology 29, 1400–1413.
Xu, X.W., Zhang, B.L., Qin, K.Z., Mao, Q., Cai, X.P., 2007d. Origin of lamprophyres by the mixing of basic and alkaline melts in magma chamber in Beiya area, western Yunnan, China. Lithos 99, 339–362.
Xu, X.W., Jiang, N., Yang, K., Zhang, B.L., Liang, G.H., Mao, Q., Li, J.X., Du, S.J., Ma, Y.G., Zhang, Y., Qin, K.Z., 2009. Accumulated phenocrysts and origin of feldspar porphyry in the Chanho area, western Yunnan, China. Lithos 113, 595–611.
Yang, Y., Hou, Z., Huang, D., Qu, X., 2002. Collision orogenic processes and magmatic metallogenic system in Zhongdian arc. Acta Geoscientia Sinica 23, 17–24 (in Chinese with English abstract).
Yunnan Bureau of Geology and Mineral Resources, 1990. Regional Geology of Yunnan Province. Beijing, Geological Publish House, p. 728 (in Chinese with English abstract).
Zeng, P.S., Mo, X., Yu, X.H., Hou, Z.Q., Xu, Q.D., Wang, H.P., Li, L.H., Yang, C.Z., 2003. Porphyries and porphyry copper deposits in Zhongdian area, northwestern Yunnan. Mineral Deposits 22, 393–400 (in Chinese with English abstract).
Zeng, P.S., Hou, Z.Q., Li, L.H., Qu, W.J., Wang, H.P., Li, W.C., Meng, Y.F., Yang, Z.S., 2004. Age of the Pulang porphyry copper deposit in NW Yunnan and its geological significance. Regional Geology of China 23, 1127–1131 (in Chinese with English abstract).
Zeng, P.S., Li, W.C., Wang, H.P., Li, L.H., 2006. The Indosinan Pulang superlarge porphyry copper deposit in Yunnan, China: petrology and chronology. Acta Petrologica Sinica 22, 989–1000 (in Chinese with English abstract).
Zhang, Y., Xie, Y., Qiu, H., Li, X., Chung, S., 1998. Shoshonitic series: Sr, Nd, and Pb isotopic compositions of ore-bearing porphyry for Yulong Cu orebelt in the eastern Xizang. Scientia Geologica Sinica 33, 359–366 (in Chinese with English abstract).
Zhao, Z., 1995. Mineralization model of Indosinan porphyry Cu–Mo deposits in the Zhongdian area. Yunnan Geology 17, 343–349 (in Chinese with English abstract).